

Microstructure and Mechanical Properties of TiB₂-HfC Ceramic Tool Materials

JINPENG SONG^{1,2,3}, JUNCAI XIE^{1,2}, MING LV^{1,2}, JIAOJIAO GAO^{1,2}
and JING AN^{1,2}

1.—School of Mechanical Engineering, Taiyuan University of Technology, Taiyuan 030024, China. 2.—Shanxi Key Laboratory of Precision Machining, The Shanxi Science and Technology Department, Taiyuan University of Technology, Taiyuan 030024, China. 3.—e-mail: songjinpeng@tyut.edu.cn

Effects of different metallic additives and sintering parameters on microstructure and mechanical properties of TiB₂-HfC ceramics were investigated. The results showed that the core-rim structure and HfC particle dispersion were discovered in these ceramics. Only Co as the metallic additive could more easily promote the formation of the strip-shaped TiB₂ than the others; TiB₂-HfC-Ni-Mo ceramic had more serious agglomeration of HfC particles than the others; for TiB₂-HfC ceramic, using Ni-Co as the metallic additive could obtain better mechanical properties than using the others. In addition, with sintering temperature increasing from 1500°C to 1650°C, grains grew gradually and the core-rim structures became fewer and unobvious. Extending the holding time from 15 min to 60 min, grain size just had a slight increase, and the influence of holding time on mechanical properties was not significant. The increase of sintering temperature (1500–1650°C) could lead to more obvious grain growth and change of core-rim structure than the increase of holding time (15–60 min). The better sintering parameters for TiB₂-HfC-Ni-Co ceramic were 1600°C and 30 min. Besides, better mechanical properties of TiB₂-HfC-Ni-Co ceramic sintered at 1600°C with 30 min holding time were that Vickers hardness was 21.2 ± 0.3 GPa, flexural strength was 1169 ± 16 MPa, and fracture toughness was 6.7 ± 0.3 MPa m^{1/2}. Meanwhile, its toughening mechanisms included core-rim structure, particle dispersion, crack deflection and crack bridging. The mixed intergranular/transgranular fracture could also improve fracture toughness.

INTRODUCTION

Titanium diboride (TiB₂) with a high melting point, high hardness, outstanding electrical and thermal properties, excellent oxidation and corrosion resistance has been widely used in the mechanical engineering field.^{1–4} Especially because of its excellent wear resistance, finishing properties and lower costs, it is a possibility for TiB₂ ceramic cutting tool material to replace the traditional WC-Co cemented carbide.⁵ However, the high densification of monolithic TiB₂ is restrained because of its low self-diffusion coefficient caused by the covalent bond between B and B atoms and electrovalent bond between B and Ti atoms.⁶ Generally, increasing the sintering temperature and extending the holding

time are methods to obtain full densification of the monolithic TiB₂. However, these will lead to the formation of abnormal grain growth and microcracks that are harmful to the improvement of mechanical properties.

To improve the sinterability of TiB₂ ceramics, metallic additives as sintering aids are often added to lower the sintering temperature and densify the ceramic. Fu et al.⁵ claimed that appropriate content of metallic additives such as Ni, Co and Mo can promote the sintering process, lower the sintering temperature and improve the sinterability of TiB₂ ceramics. Chlupa et al.⁷ refined the microstructure and improved the flexural strength of TiB₂ ceramics by adding Ni and Ta metallic additives. Besides, metallic additives can improve the density of

material because in the sintering process they will melt into liquid phase and fill into pores. Therefore, it is important to select the appropriate metallic additive to improve the sinterability, microstructure and mechanical properties of TiB₂ ceramics.

Besides metallic additives, strengthening phases are usually employed to improve the flexural strength of TiB₂ ceramics. Koide et al.⁸ improved the flexural strength of TiB₂ ceramics by adding a TiN additive that can inhibit TiB₂ grain growth and reinforce the grain boundary between TiB₂ and TiN. Gu et al.⁹ added Al₂O₃ into TiB₂ ceramics to promote the densification and improve the flexural strength of TiB₂-based ceramics. In our previous work, we found that HfC can also accelerate the densification of TiB₂-based ceramics and inhibit TiB₂ grain growth.¹⁰

In addition, sintering parameters also influence the microstructure and mechanical properties of ceramic tool materials. Generally, higher sintering temperature and longer holding time result in coarse grains that lower the mechanical properties significantly. Zou et al.¹¹ investigated the effects of sintering parameters on TiB₂-based ceramics and showed that the improvement of mechanical properties resulted from a shorter holding time. Gu et al.⁶ indicated that with an increase of sintering temperature and extension of holding time, the grain size and density of TiB₂-based ceramic increased, which resulted in higher fracture toughness. Hence, the microstructure and mechanical properties of TiB₂-based ceramics can be ameliorated by controlling the sintering parameters.

So, based on our previous work on TiB₂-HfC ceramics,¹⁰ this article will further investigate the influence of metallic additives and sintering parameters on the microstructure and mechanical properties of TiB₂-HfC ceramics. These ceramics will be fabricated by the conventional powder metallurgical method with vacuum hot-pressing sintering technology.

EXPERIMENTAL PROCEDURE

Commercially available TiB₂ (> 99%, 1 μm, Shanghai Xiangtian Nanomaterials Co., Ltd., Shanghai, China) and HfC (> 99%, 0.8 μm, Shanghai Chaowei Nanomaterials Co., Ltd, Shanghai, China) were added as raw materials. Metals Ni, Co, and Mo with the average grain size of 1 μm and purity of more than 99% were added as sintering aids. The metal powders were all commercially obtained from Shanghai Yunfu Nanotechnology Co. Ltd. of China. First, this article investigated the effects of metallic additives on the microstructure and mechanical properties of TiB₂-HfC ceramics (THN: TiB₂-20 wt.% HfC-8 wt.% Ni, THC: TiB₂-20 wt.% HfC-8 wt.% Co, THNC: TiB₂-20 wt.% HfC-4 wt.% Ni-4 wt.% Co, THNM: TiB₂-20 wt.% HfC-4 wt.% Ni-4 wt.% Mo) sintered at 1650°C to obtain a better metallic additive. Second, better sintering

temperature would be obtained through investigating the microstructure and mechanical properties of TiB₂-HfC ceramics with the better metallic additive under different sintering temperatures (1500°C, 1550°C, 1600°C, and 1650°C). Third, better holding time would be obtained by investigating the microstructure and mechanical properties of TiB₂-HfC ceramics with the better metallic additive and sintering temperature under different holding times (15 min, 30 min, 45 min, and 60 min).

Mixed raw materials were milled for 48 h in a polyethylene jar with WC balls and alcohol as mediums. Then, the mixed slurry was dried in vacuum and sieved by a 200-mesh sieve. Compacted powders were hot pressed under 30 MPa in a vacuum (3×10^{-3} Pa), and the heating rate was 30°C/min to the final temperature. Hot-pressing sintered samples were cut by an electric spark wire cutting machine, then ground and polished, and their dimensions were 3 mm × 4 mm × 40 mm. Ten specimens were tested for each experimental condition.

According to Chinese National Standards GB/T 6569-2006/ISO 14704: 2000,¹² flexural strength was measured at a span of 30 mm and across a head speed of 0.5 mm/min by the three-point bending test method on an electron universal tester. Fracture toughness (K_{IC}) was calculated using the equation² as follows:

$$K_{IC} = 0.203H_V a^{1/2} \left(\frac{c}{a}\right)^{-3/2}$$

Based on Chinese National Standards GB/T 16534-2009,¹³ Vickers hardness was measured on polished surfaces using a diamond pyramid indenter under a load of 196 N for 15 s by HV-120. Density was measured by the Archimedes method with distilled water as the medium. Relative density was the ratio of the measured density to the theoretical density. Microstructure and compositions of the composites were observed by x-ray diffraction (XRD, EMPYREAN, PANalytical B.V., Almelo, The Netherlands), an energy dispersive spectrometer (EDS, ACT-350, Oxford Instruments, Oxford, UK) and scanning electron microscope (SEM, Supra-55, Carl Zeiss AG, Germany).

RESULTS AND DISCUSSIONS

Microstructure and Mechanical Properties of TiB₂-HfC Ceramics Influenced by Different Metallic Additives

Microstructure of TiB₂-HfC Ceramics Sintered at 1650°C for 30 min with Different Metallic Additives

Figure 1 shows XRD patterns of TiB₂-HfC ceramics sintered at 1650°C for 30 min with different metallic additives (Ni, Co, Ni-Co, and Ni-Mo). Major crystal phases were TiB₂, HfC and the corresponding metallic additives in these ceramics. Some by-

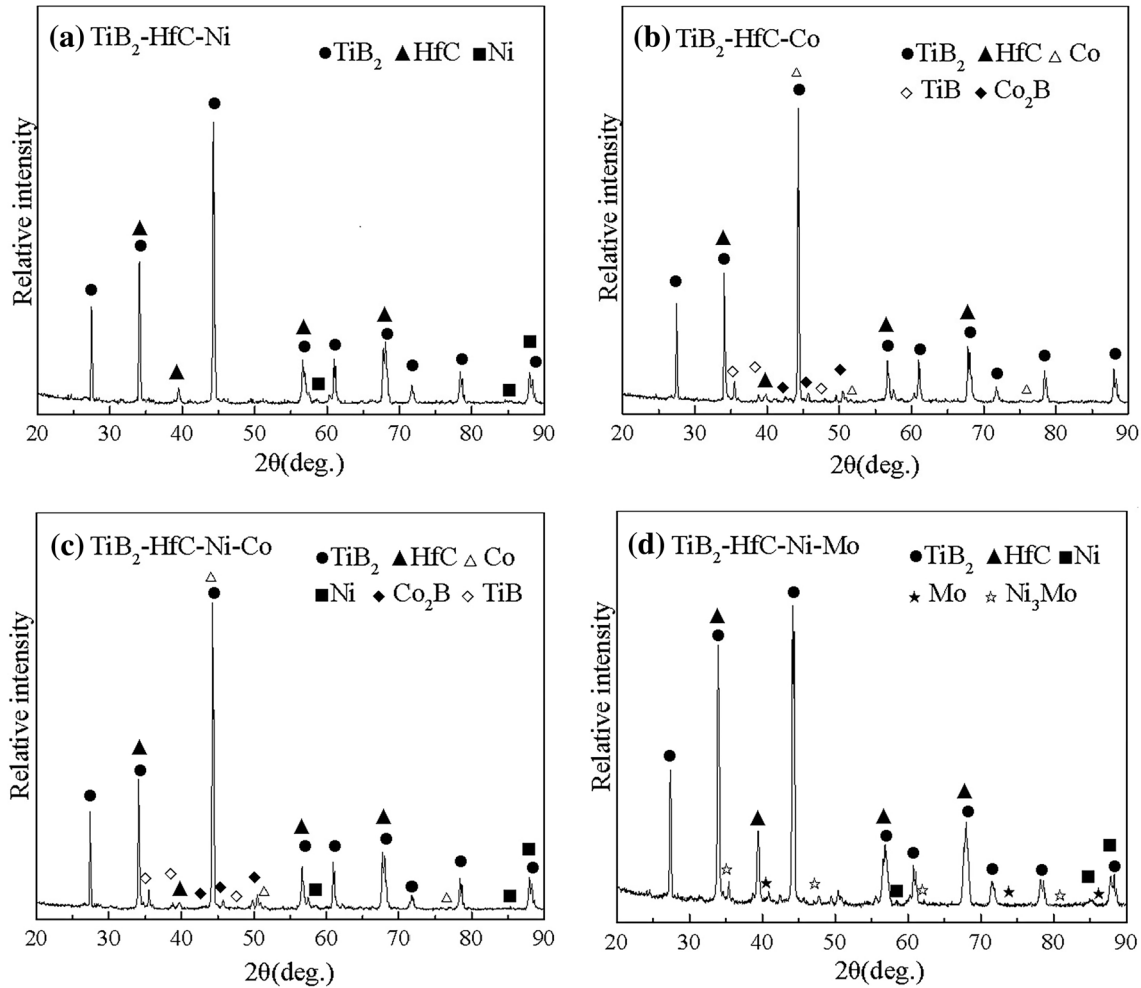


Fig. 1. XRD patterns of TiB_2 -HfC ceramics sintered at 1650°C for 30 min with different metallic additives: (a) THN, (b) THC, (c) THNC and (d) THNM.

products (TiB and Co_2B in THC and THNC ceramics, Ni_3Mo in THNM ceramic) were generated in these ceramics except THN ceramic. In THC and THNC ceramics, TiB and Co_2B were generated through reaction 1, which could take place at 1650°C through thermodynamic calculation. According to the XRD results in Fig. 1b and c, the residual Co showed that a slight reaction occurred in THC and THNC ceramics. The slight reaction between the metal and ceramic to some extent could improve the grain boundary strength for ceramics.¹⁴ Sánchez et al.¹⁵ indicated that Co could react with TiB_2 to form metal borides of the M_2B type. Besides, metal borides such as Co_2B and TiB had good mechanical properties such as high thermal and electrical conductivity, good wear resistance, a high melting point and high hardness.¹⁶ Ni_3Mo was discovered in THNM ceramic. Khalfallah et al.¹⁷ reported that Ni and Mo could form Ni_3Mo intermetallic compound at 1300°C . In addition, reaction 2 could also take place at 1650°C ; however, there were no obvious diffraction peaks of HfB_2 and TiC detected in XRD patterns. This indicated that the

reaction between TiB_2 and HfC was too weak in the sintering process. Compared with the standard PDF card, HfC diffraction peaks shifted about 1° to the right, which led to the overlapped HfC and TiB_2 peaks. This indicated that the exchange of Ti and Hf atoms probably occurred during the sintering process, which would lead to the formation of a complex solid solution of TiB_2 and HfC in these ceramics.

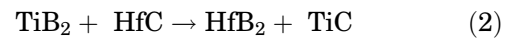
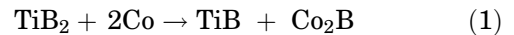


Figure 2 exhibits SEM micrographs of polished surfaces of TiB_2 -HfC ceramics sintered at 1650°C for 30 min with different metallic additives (Ni, Co, Ni-Co, and Ni-Mo). There were three distinct phases, namely a black, white and gray phase, as shown in Fig. 2. Based on our previous work,¹⁰ the black phase was a refractory TiB_2 grain and the white phase was mainly composed of HfC in all ceramics. For obtaining compositions of the gray phase in TiB_2 -HfC ceramics, it was necessary to determine the formation of the typical core-rim structure (indicated by

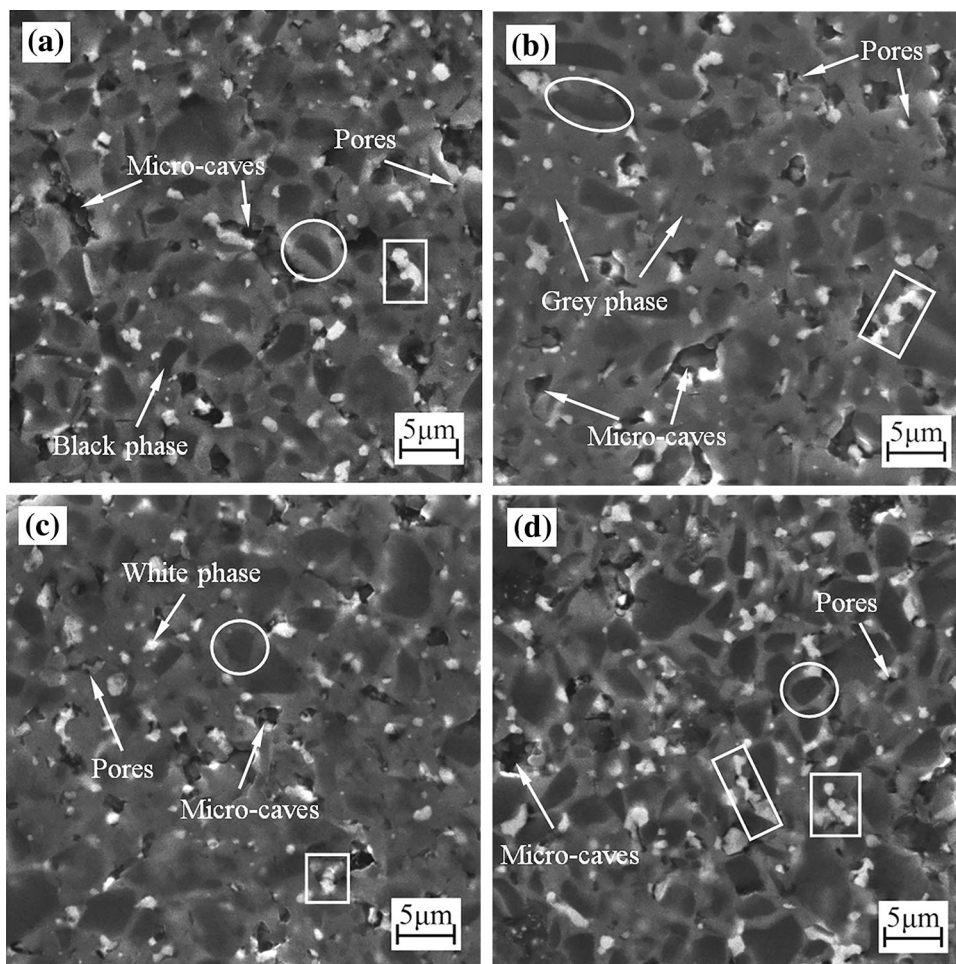


Fig. 2. SEM micrographs of polished surfaces of $\text{TiB}_2\text{-HfC}$ ceramics sintered at 1650°C for 30 min with different metallic additives: (a) THN, (b) THC, (c) THNC and (d) THNM.

the circles in Fig. 2). Formation of the core-rim structure was derived from the dissolution-precipitation process: with sintering temperature increasing, metallic additives melted into liquid; meanwhile, under high temperature, molecular motion would become stronger and, TiB_2 and HfC particles would dissolve into the metal liquid and form new materials with liquid metal; during the cooling stage, newly formed materials would wrap around TiB_2 grains to form the core-rim structure during the precipitation process. Therefore, the core consisted of refractory TiB_2 grain; besides the complex solid solution, the rim (the gray phase) included Ni in THN ceramic, Co, Co_2B , and TiB in THC ceramic, Ni, Co, Co_2B , and TiB in THNC ceramic and Ni, Mo, and Ni_3Mo in THNM ceramic. To some extent, the rim phase probably could isolate the amalgamation of TiB_2 grains and then inhibit the core growth effective to refine TiB_2 grains.

In addition, micro-voids were discovered in Fig. 2-a, b, c, and d. These micro-voids were composed of pores and micro-caves as shown in Fig. 2. Pores forming in the sintering process were the source of

crack and harmful to mechanical properties, especially to flexural strength and fracture toughness. Due to the weak grain boundary strength, micro-caves were left by the detached grains during the grinding and polishing process. It was obvious that there were more micro-voids in THN and THC ceramics than in THNC and THNM ceramics and that micro-voids were bigger in THN and THC ceramics. These indicated that Ni-Co and Ni-Mo as binder phase had better wettability with ceramic phase. Besides, HfC particles were mainly distributed in the gray phase. HfC particles dispersed more uniformly and were finer in THNC than in the others. However, there was more serious agglomeration (indicated by the rectangles in Fig. 2d) of HfC in THNM than in the others. The agglomeration was probably caused by the less metal liquid.

Figure 3 displays fracture morphologies of $\text{TiB}_2\text{-HfC}$ ceramics sintered at 1650°C for 30 min with different metallic additives. Some white dots (indicated by the solid arrows in Fig. 3) of about $1\ \mu\text{m}$ were HfC particles dispersing in these ceramics. Ying et al.¹⁸ pointed out that particle dispersion could

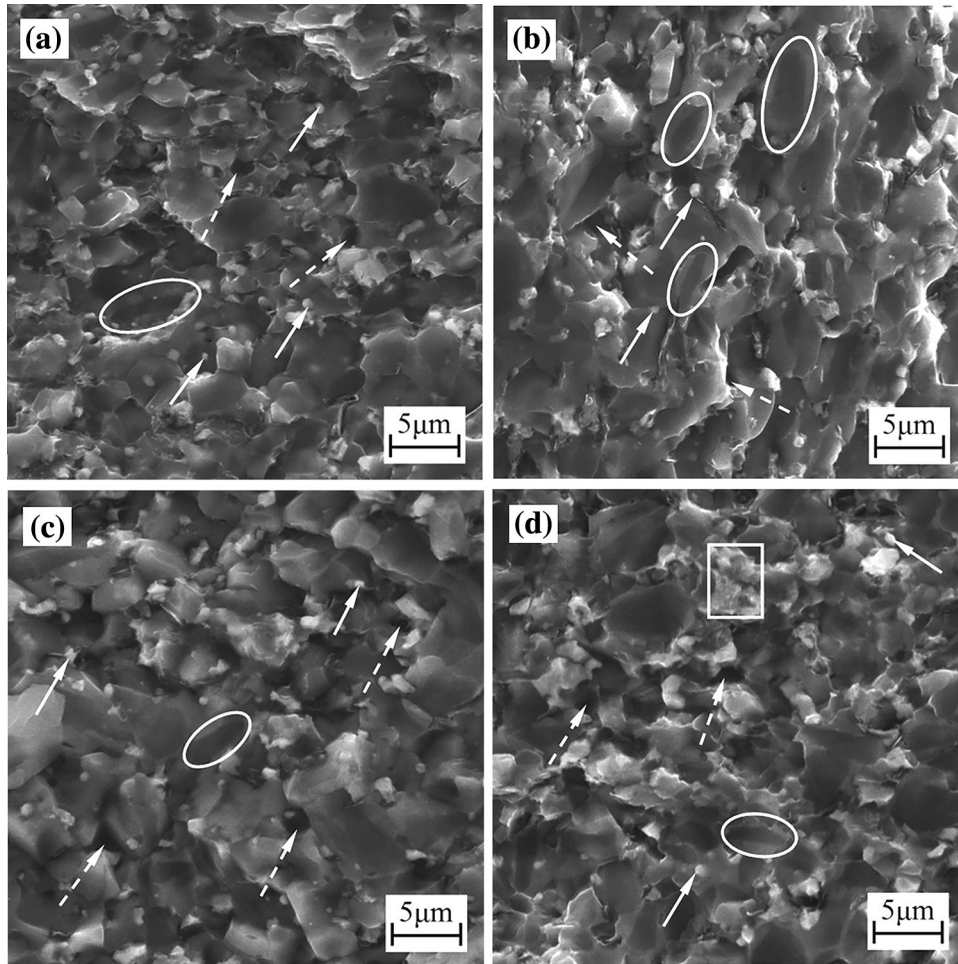


Fig. 3. Fracture morphologies of $\text{TiB}_2\text{-HfC}$ ceramics sintered at 1650°C for 30 min with different metallic additives: (a) THN, (b) THC, (c) THNC and (d) THNM.

improve the mechanical properties and thermal conductivity coefficient of ceramic tool materials and then enhance the cutting performance and tool life. In Fig. 3d, HfC particles showed serious agglomeration (indicated by the rectangles in Fig. 3d) in THNM ceramic. This serious agglomeration was harmful to the improvement of mechanical properties. As can be seen, pits (indicated by the dashed arrow in Fig. 3) left by pulled out grains were discovered in each ceramic. Pulled out grains were a benefit for the improvement of flexural strength. In addition, the typical core-rim structure (indicated by circles) was also discovered in these ceramics (Fig. 3). In THC there was more strip-shaped TiB_2 with a large aspect ratio, which indicated that only Co as a metallic additive could more easily promote the formation of strip-shaped TiB_2 than the others. This shape was different from the block shape of TiB_2 with a small aspect ratio reported in the literature.¹⁹ The strip-shaped TiB_2 in THC ceramic was probably advantageous to enhance the mechanical properties of the ceramic.

Figure 4 exhibits SEM micrographs of crack propagation paths of $\text{TiB}_2\text{-HfC}$ ceramics sintered at 1650°C for 30 min with different metallic additives. Crack propagation paths were straighter in THN and THNM ceramics than in THC and THNC ceramics, which indicated that the gray phases in THN and THNM ceramics were more fragile than those in THC and THNC ceramics. Transgranular fracture was discovered in THN and THNM ceramics. Besides, crack bridging was discovered in THNM ceramic. The formation of this transgranular fracture involved cracks traversing big TiB_2 grains. Transgranular fracture, intergranular fracture and crack deflection were discovered in THC and THNC ceramics. In THNC ceramic, crack bridging took place more times, which indicated the stronger grain boundary strength formed in THNC ceramic under the synergistic effect of Ni and Co. In addition, Gao et al.²⁰ illustrated that the coexistence of intergranular fracture and transgranular fracture was advantageous to the improvement of flexural strength and fracture toughness.

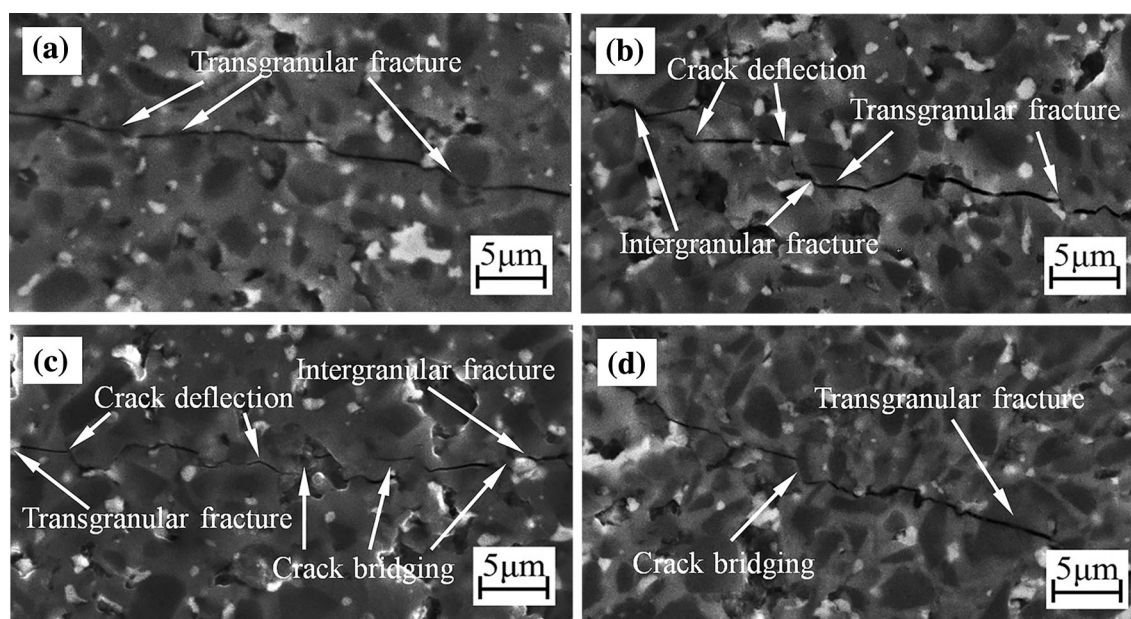


Fig. 4. SEM micrographs of crack propagation paths of TiB₂-HfC ceramics sintered at 1650°C for 30 min with different metallic additives: (a) THN, (b) THC, (c) THNC and (d) THNM.

Relative Density and Mechanical Properties of TiB₂-HfC Ceramics Sintered at 1650°C for 30 min with Different Metallic Additives

Relative density was $89.9 \pm 0.2\%$ for THN ceramic, $99.0 \pm 0.2\%$ for THC ceramic, $99.6 \pm 0.1\%$ for THNC ceramic and $99.1 \pm 0.1\%$ for THNM ceramic, respectively. It was clear that the relative density of THN and THC was lower than that of THNC and THNM. Relative density was closely related to the porosity of materials. Lower porosity led to higher relative density. The pore number in THN and THC ceramics was more than that in THNC and THNM ceramics, as shown in Fig. 2. This illustrated that Ni-Co and Ni-Mo were more beneficial to enhancing the densification of TiB₂-HfC ceramics.

Vickers hardness was 17.4 ± 0.3 GPa for THN ceramic, 21.3 ± 0.2 GPa for THC ceramic, 22.8 ± 0.3 GPa for THNC ceramic and 19.3 ± 0.2 GPa for THNM ceramic, respectively. Generally, higher relative density resulted in higher Vickers hardness. THNC ceramic obtained the highest Vickers hardness (22.8 ± 0.3 GPa), which was mainly due to the highest relative density and the high hardness of Co₂B and TiB₁₆. However, THC ceramic with lower relative density obtained higher Vickers hardness (21.3 ± 0.2 GPa), probably because of the more strip-shaped TiB₂ in this ceramic. THNM ceramic with higher relative density obtained lower Vickers hardness (19.3 ± 0.2 GPa), probably because of the agglomeration of HfC and the brittle gray phase. THN ceramic had the lowest Vickers hardness (17.4 ± 0.3 GPa) because of the lowest relative density and brittle gray phase.

Flexural strength was 692 ± 25 MPa for THN ceramic, 721 ± 19 MPa for THC ceramic, 834 ± 24 MPa for THNC ceramic and 795 ± 22 MPa for THNM ceramic, respectively. The flexural strength of THC ceramic was slightly higher than that of THN ceramic due to the higher grain boundary strength, which was caused by the slight reaction between Co and TiB₂ in THC. The flexural strength of THNM ceramic was higher than that of THN and THC ceramics due to the fewer micro-voids in THNM ceramic. THNC ceramic had the highest flexural strength, which was mainly due to the coexistence of inter- and transgranular fracture, homogeneously distributed HfC particles and the stronger grain boundary strength.

Fracture toughness was 7.7 ± 0.2 MPa m^{1/2} for THN ceramic, 9.5 ± 0.3 MPa m^{1/2} for THC ceramic, 9.5 ± 0.3 MPa m^{1/2} for THNC ceramic and 7.5 ± 0.2 MPa m^{1/2} for THNM ceramic, respectively. The fracture toughness of THNM ceramic was the lowest, mainly because of the serious agglomeration of HfC particles caused by less metal liquid and the straight crack propagation caused by the brittle gray phase. The fracture toughness of THN ceramic was lower, mainly because of more micro-voids and the straight crack propagation. The fracture toughness of THC and THNC ceramics was the highest, mainly owing to the zigzag crack propagation, crack deflection and combination of transgranular fracture and intergranular fracture. Besides, for THNC ceramic, crack bridging also had a positive effect on improving the fracture toughness. Based on the above analysis, THNC ceramic obtained better mechanical properties than the others, which indicated that the better metallic additive for TiB₂-HfC ceramic was Ni-Co.

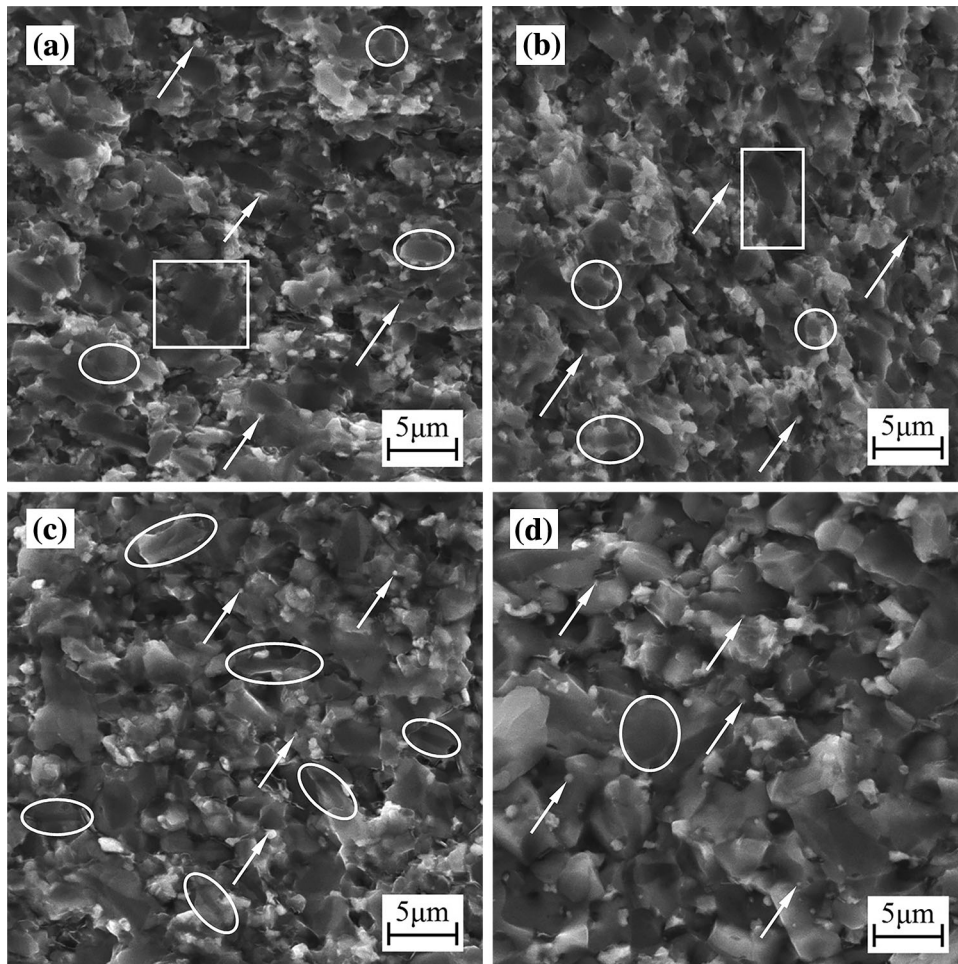


Fig. 5. Fracture morphologies of $\text{TiB}_2\text{-HfC-Ni-Co}$ ceramics sintered at different sintering temperatures with holding time of 30 min: (a) 1500°C , (b) 1550°C , (c) 1600°C , and (d) 1650°C .

Microstructure and Mechanical Properties of $\text{TiB}_2\text{-HfC-Ni-Co}$ Ceramics Influenced by Sintering Temperatures

Microstructure of $\text{TiB}_2\text{-HfC-Ni-Co}$ Ceramics Sintered at Different Temperatures (1500°C , 1550°C , 1600°C , and 1650°C)

Figure 5 displays fracture morphologies of $\text{TiB}_2\text{-HfC-Ni-Co}$ ceramics sintered at different sintering temperatures. With increasing sintering temperature, grains grew gradually and the core-rim structures became fewer and unobvious. The reason was that the diffusion between atoms became stronger leading to the acceleration of the reaction between Co and TiB_2 and the formation of the complex solid solution of HfC and TiB_2 . When sintering temperatures were 1500°C and 1550°C , shown in Fig. 5a and b, there were numerous cores and some big cores (as marked by rectangles). These big cores made the microstructure uneven. The reason was that at the lower sintering temperature (1500°C and 1550°C), the slow atom diffusion reduced the consumption of TiB_2 . These indicated that 1500°C and 1550°C were too low for $\text{TiB}_2\text{-HfC-Ni-Co}$ ceramic to

obtain a better microstructure. While the sintering temperature was 1600°C , big cores were undiscovered and more strip-shaped TiB_2 grains with big aspect ratios were discovered. These strip-shaped TiB_2 grains were homogeneously distributed. When the sintering temperature was 1650°C , there were few cores and many coarse grains, as shown in Fig. 5d. These indicated that 1650°C was too high for $\text{TiB}_2\text{-HfC-Ni-Co}$ ceramic to obtain a better microstructure. Excessively high sintering temperature could result in the formation of coarse grains that were harmful to the improvement of flexural strength. Gu et al.⁶ stated that the coarse grains could induce micro-cracks and then decrease the flexural strength.

Relative Density and Mechanical Properties of $\text{TiB}_2\text{-HfC-Ni-Co}$ Ceramics Sintered at Different Temperatures (1500°C , 1550°C , 1600°C , and 1650°C)

Relative density of $\text{TiB}_2\text{-HfC-Ni-Co}$ ceramics sintered at different temperatures was $99.1 \pm 0.2\%$ (1500°C), $99.2 \pm 0.1\%$ (1550°C), $99.5 \pm 0.2\%$ (1600°C) and $99.6 \pm 0.1\%$ (1650°C), respectively.

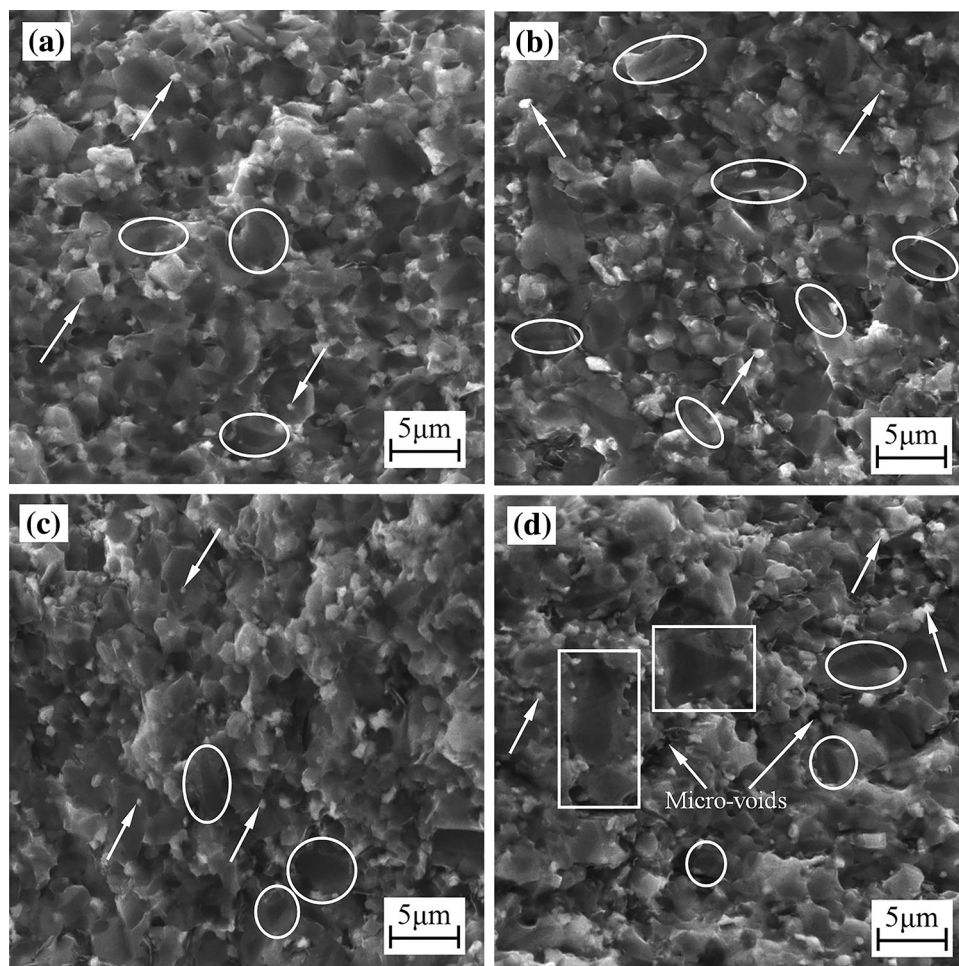


Fig. 6. Fracture morphologies of TiB₂-HfC-Ni-Co ceramics sintered at 1600°C with different holding times: (a) 15 min, (b) 30 min, (c) 45 min, and (d) 60 min.

With increasing sintering temperature, relative density increased gradually, consistent with the result of the paper.⁶ This was because, with the sintering temperature increasing, the flow of metal liquid accelerated and liquid metal filled into gaps among grains. High relative density was beneficial to the mechanical properties such as Vickers hardness, flexural strength and fracture toughness.

Vickers hardness was 15.1 ± 0.3 GPa (1500°C), 16.7 ± 0.3 GPa (1550°C), 21.2 ± 0.3 GPa (1600°C), and 22.8 ± 0.3 GPa (1650°C), respectively. With increasing sintering temperature, Vickers hardness increased gradually. The variation of Vickers hardness was consistent with the variation of relative density as the sintering temperature increased. When the sintering temperature increased from 1550°C to 1600°C, the hardness significantly improved, which was mainly attributed to the more homogeneously distributed strip-shaped TiB₂ grains with a big aspect ratio. However, when the sintering temperatures were 1500°C and 1550°C, the lower Vickers hardnesses were mainly due to the big cores. The highest Vickers hardness of TiB₂-HfC-Ni-

Co ceramic sintered at 1650°C was mainly ascribed to its highest relative density.

Flexural strength was 974 ± 26 MPa (1500°C), 1080 ± 22 MPa (1550°C), 1169 ± 16 MPa (1600°C), and 834 ± 24 MPa (1650°C), respectively. Flexural strength increased first and then decreased with the sintering temperature increasing from 1500°C to 1650°C. The maximum of flexural strength was 1169 ± 16 MPa when the sintering temperature was 1600°C. When the sintering temperature increased from 1500°C to 1600°C, the flexural strength increased gradually, because the liquid metal uniformly filled into the gaps among grains and then strengthened the grain boundary. The ceramic sintered at 1600°C had the highest flexural strength due to its higher relative density and more homogeneously distributed strip-shaped TiB₂ grains with a big aspect ratio. With the sintering temperature increasing to 1650°C, the flexural strength decreased dramatically, which was mainly ascribed to the formation of more coarse grains. Coarse grains not only could induce micro-cracks, but also could generate strength concentration; these were harmful to flexural strength.

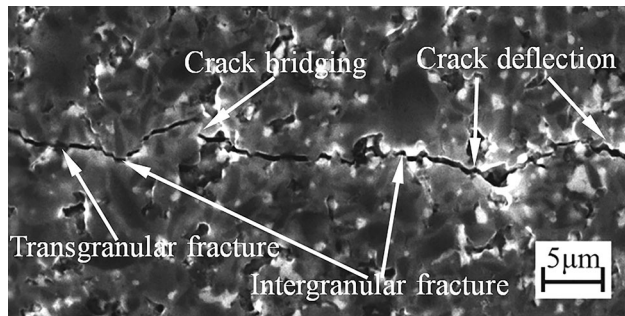


Fig. 7. SEM micrograph of crack propagation path of $\text{TiB}_2\text{-HfC-Ni-Co}$ ceramic sintered at 1600°C with holding time of 30 min.

Fracture toughness was $5.9 \pm 0.2 \text{ MPa m}^{1/2}$ (1500°C), $6.3 \pm 0.2 \text{ MPa m}^{1/2}$ (1550°C), $6.7 \pm 0.3 \text{ MPa m}^{1/2}$ (1600°C), and $9.5 \pm 0.3 \text{ MPa m}^{1/2}$ (1650°C), respectively. With sintering temperature increasing from 1500°C to 1650°C , fracture toughness increased gradually. When the sintering temperature increased from 1500°C to 1600°C , the improvement of fracture toughness was not obvious. While the sintering temperature increased to 1650°C , fracture toughness had a significant improvement. The reason was that with the sintering temperature increasing, the flow of the metal liquid accelerated and more grains were wetted, so the grain boundary strength was enhanced. In addition, the ceramic sintered at 1650°C had coarse grains. Gu et al.⁶ indicated that coarse grains could impede crack propagation and to some extent could change the crack propagating direction to form crack deflection. Crack deflection could consume much fracture energy and then enhance the fracture toughness of ceramics.

Microstructure and Mechanical Properties of $\text{TiB}_2\text{-HfC-Ni-Co}$ Ceramics Sintered at 1600°C Influenced by Different Holding Times

Microstructure of $\text{TiB}_2\text{-HfC-Ni-Co}$ ceramics sintered at 1600°C with different holding times (15 min, 30 min, 45 min, and 60 min)

Based on the above analysis, $\text{TiB}_2\text{-HfC-Ni-Co}$ ceramic sintered at 1600°C had better microstructure and higher flexural strength and Vickers hardness. Therefore, 1600°C was selected as the sintering temperature for fabricating $\text{TiB}_2\text{-HfC-Ni-Co}$ ceramics, and effects of different holding time on their microstructure and mechanical properties were further investigated. Figure 6 shows the fracture morphologies of $\text{TiB}_2\text{-HfC-Ni-Co}$ ceramics sintered at 1600°C with different holding times. Particle dispersion (indicated by arrows) and the typical core-rim structure (as marked by circles) were still discovered in these ceramics. The average grain size just had a slight increase with the extension of holding time, consistent with the result

of the investigation.²¹ Grains were the finest and more homogeneous in Fig. 6a and were coarsest in Fig. 6d. Meanwhile, as shown in Fig. 6, with holding time increasing from 15 min to 60 min, the aspect ratio of strip-shaped TiB_2 grains (as marked by circles) increased first and then decreased. It had the biggest value when the holding time was 30 min, shown in Fig. 6b. Extending the holding time from 15 min to 60 min, the time of liquid sintering became longer, so the reaction and diffusion among atoms, and the dissolution-precipitation process, became more complete. Better holding time would promote the formation of more strip-shaped TiB_2 grains. However, an overlong holding time would result in the formation of coarse grains (as marked by rectangles in Fig. 6d) and micro-voids (as marked in Fig. 6d) that were disadvantageous for improving the Vickers hardness and flexural strength. With the overlong holding time, the complete reaction would consume more metal liquid. At the cooling stage, the shrinkage of grains would result in the formation of micro-voids because of the lack of metal liquid.

In this investigation, based on previous analyses and results, in contrast with the holding time (15–60 min), the sintering temperature ($1500\text{--}1650^\circ\text{C}$) showed an obvious influence on the microstructure: the increase of sintering temperature ($1500\text{--}1650^\circ\text{C}$) could lead to more obvious grain growth and change of core-rim structure than the increase of holding time (15–60 min), because the high sintering temperature could provide more energy to promote grain growth, liquid flow and atom diffusion than the long holding time.

Relative Density and Mechanical Properties of $\text{TiB}_2\text{-HfC-Ni-Co}$ Ceramics Sintered at 1600°C with Different Holding Times (15 min, 30 min, 45 min, and 60 min)

Relative density of $\text{TiB}_2\text{-HfC-Ni-Co}$ ceramics sintered at 1600°C with different holding times was $99.6 \pm 0.1\%$ (15 min), $99.5 \pm 0.2\%$ (30 min), $99.5 \pm 0.1\%$ (45 min), and $99.4 \pm 0.3\%$ (60 min), respectively. When the holding time was 60 min, the lowest relative density was mainly ascribed to the presence of the micro-voids. As can be seen, the difference of their relative density was very small. This indicated that the effect of holding time from 15 min to 60 min on relative density was not significant. Lóh et al.²¹ also showed that the influence of holding time on relative density and mechanical properties was not significant. Vickers hardness was $22.1 \pm 0.6 \text{ GPa}$ (15 min), $21.2 \pm 0.3 \text{ GPa}$ (30 min), $19.2 \pm 0.3 \text{ GPa}$ (45 min), and $18.4 \pm 0.2 \text{ GPa}$ (60 min), respectively. Extending the holding time, Vickers hardness decreased gradually. The reason was mainly that with extending the holding time, by-products increased, and their hardness was lower than that of TiB_2 . When the holding time was 60 min, the ceramic had the

lowest Vickers hardness of 18.4 ± 0.2 GPa mainly due to the more micro-voids and by-products.

Flexural strength was 1057 ± 18 MPa (15 min), 1169 ± 16 MPa (30 min), 1023 ± 20 MPa (45 min), and 998 ± 13 MPa (60 min), respectively. Extending the holding time from 15 min to 60 min, flexural strength increased first and then decreased. When the holding time was 15 min, the ceramic had higher flexural strength due to the finest and more homogeneous distributed grains. When the holding time was 30 min, the ceramic had the highest flexural strength, which was mainly due to strip-shaped TiB₂ grains with a bigger aspect ratio. Compared with the flexural strength of ceramic with 30-min holding time, flexural strength of ceramic with 45 min was lower mainly owing to the strip-shaped TiB₂ grains with smaller aspect ratios and bigger grain sizes. When the holding time was 60 min, the ceramic had the lowest flexural strength owing to the coarsest grains and micro-voids.

Fracture toughness was 6.0 ± 0.1 MPa m^{1/2} (15 min), 6.7 ± 0.3 MPa m^{1/2} (30 min), 5.3 ± 0.2 MPa m^{1/2} (45 min), and 5.2 ± 0.4 MPa m^{1/2} (60 min), respectively. Fracture toughness increased first and then decreased. Generally, higher grain boundary strength can improve the fracture toughness of ceramics. When the holding time was 30 min, the ceramic had the highest fracture toughness, which demonstrated higher grain boundary strength could be obtained with 30-min holding time. When the holding time was shorter, the reaction was too weak to obtain higher grain boundary strength. When the holding time was longer, the reaction was too strong, resulting in less metal liquid. Less metal liquid could deteriorate the grain boundary and lead to the generation of micro-voids. Therefore, too short and too long holding times were disadvantageous to improve fracture toughness.

Based on the above analysis, TiB₂-HfC-Ni-Co ceramic sintered at 1600°C for 30 min obtained better comprehensive mechanical properties. To further determine the toughening mechanisms of ceramic sintered at 1600°C for 30 min, the crack propagation path is exhibited in Fig. 7. The TiB₂ grain as a bridge connected the crack to form crack bridging. The TiB₂ grain as the bridge could provide great resistance in the crack propagation path and then consume much of the fracture energy. The coexistence of crack bridging and crack deflection could greatly enhance the fracture toughness. Therefore, the toughening mechanisms of TiB₂-HfC-Ni-Co ceramic sintered at 1600°C for 30 min were particle dispersion, crack deflection and crack bridging. In addition, the mixed intergranular/transgranular fracture was also advantageous to the improvement of fracture toughness.

CONCLUSION

TiB₂-HfC ceramics were fabricated by vacuum hot-pressing sintering. Effects of metallic additives and sintering parameters on the microstructure and mechanical properties were investigated. The conclusions were as follows:

1. TiB and Co₂B were discovered in TiB₂-HfC ceramics with Co and Ni-Co as metallic additives, and Ni₃Mo was discovered in TiB₂-HfC ceramics with Ni-Mo as metallic additive. Core-rim structure and HfC particle dispersion were discovered in these ceramics; only Co as the metallic additive could more easily promote the formation of strip-shaped TiB₂ than the others; TiB₂-HfC-Ni-Mo ceramic had more serious agglomeration of HfC than the others. Ni-Co was the better metallic additive for TiB₂-HfC ceramic.
2. With the sintering temperature increasing from 1500°C to 1650°C, grains grew gradually and the core-rim structures became fewer and unobvious. Meanwhile, Vickers hardness and fracture toughness increased gradually, and the flexural strength increased first and then decreased. When the sintering temperature was 1600°C, big cores were undiscovered and more strip-shaped TiB₂ grains with big aspect ratios were distributed homogeneously. The better sintering temperature was 1600°C for TiB₂-HfC-Ni-Co ceramic.
3. Extending the holding time from 15 min to 60 min, grain size just had a slight increase and the influence of holding time on mechanical properties was not significant. Extending the holding time, Vickers hardness decreased gradually, and flexural strength and fracture toughness increased first and then decreased. TiB₂-HfC-Ni-Co ceramic obtained better comprehensive mechanical properties with 30 min than with 15 min, 45 min, and 60 min. The better mechanical properties of TiB₂-HfC-Ni-Co ceramic sintered at 1600°C with 30 min were that Vickers hardness was 21.2 ± 0.3 GPa, flexural strength was 1169 ± 16 MPa, and fracture toughness was 6.7 ± 0.3 MPa m^{1/2}. Its toughening mechanisms included the core-rim structure, particle dispersion, crack deflection and crack bridging. The mixed intergranular/transgranular fracture was also helpful for improving the fracture toughness.

ACKNOWLEDGEMENTS

This project is supported by National Natural Science Foundation of China (Grant Nos. 51875388 and 51405326) and Scientific and Technological Innovation Programs of Higher Education Institutions in Shanxi (Grant No. 2014122).

REFERENCES

1. R. González, M.G. Barandika, D. Oña, J.M. Sánchez, A. Villellas, A. Valea, and F. Castro, *Mater. Sci. Eng., A* 216, 185 (1996).
2. J. An, J.P. Song, G.X. Liang, J.J. Gao, J.C. Xie, L. Cao, S.Y. Wang, and M. Lv, *Materials* 10, 461 (2017).
3. B. Zou, C.Z. Huang, W.B. Ji, and S.S. Li, *Ceram. Int.* 40, 3667 (2014).
4. B. Basu, G.B. Raju, and A.K. Suri, *Int. Mater. Rev.* 51, 352 (2006).
5. Z.Z. Fu and R. Koc, *Mater. Sci. Eng., A* 676, 278 (2016).
6. M.L. Gu, H.J. Xu, J.H. Zhang, Z. Wei, and A.P. Xu, *Mater. Sci. Eng., A* 545, 1 (2012).
7. Z. Chlupa, L. Bača, M. Halasová, E. Neubauer, H. Hadraba, N. Stelzer, and P. Roupčová, *J. Eur. Ceram. Soc.* 35, 2745 (2015).
8. M. Koide, K. Jabri, A. Saito, M. Imori, and T. Sato, *J. Ceram. Soc. Jpn.* 125, 413 (2017).
9. M.L. Gu, C.Z. Huang, S.R. Xiao, and H.L. Liu, *Mater. Sci. Eng., A* 486, 167 (2008).
10. J.P. Song, L.K. Jiang, G.X. Liang, J.J. Gao, J. An, L. Cao, J.C. Xie, S.Y. Wang, and M. Lv, *Ceram. Int.* 43, 8202 (2017).
11. B. Zou, C.Z. Huang, J.P. Song, Z.Y. Liu, L. Liu, and Y. Zhao, *Mater. Sci. Eng., A* 540, 235 (2012).
12. China State Bureau of Technological Supervision, *Chinese National Standards-Fine Ceramics (Advanced Ceramics, Advanced Technical Ceramics)-Test Method for Flexural Strength of Monolithic Ceramics at Room Temperature* (Beijing: Chinese Standard Publishing House, 2006).
13. China State Bureau of Technological Supervision, *Chinese National Standards-Fine Ceramics (Advanced Ceramics, Advanced Technical Ceramics)-Test Method for Hardness of Monolithic Ceramics at Room Temperature* (Beijing: Chinese Standard Publishing House, 2009).
14. K.Q. Liu, Q. Xu, and H.J. Zhang, *Preparation and application of cermet* (Beijing: Metallurgical Industry Press, 2008).
15. J.M. Sánchez, I. Azcona, and F. Castro, *J. Mater. Sci.* 35, 9 (2000).
16. H.J. Liu, Y. Pan, W.M. Guan, K.H. Zhang, C.P. Yin, and Y.L. Du, *Chin. J. Rare Mater.* 37, 633 (2013).
17. I. Khalfallah and A. Aning, *TMS 143rd Annual Meeting and Exhibition*, vol. 999 (2014).
18. J.X. Ying, X.M. Pang, J.Q. Zhou, L.J. Qian, and S.S. Lin, *J. Mech. Electr. Eng.* 33, 973 (2016).
19. L. Ma, J.C. Yu, X. Guo, B.Y. Xie, H.Y. Gong, Y.J. Zhang, Y.X. Zhai, and X.Z. Wu, *Ceram. Int.* 44, 4491 (2018).
20. J.J. Gao, J.P. Song, G.X. Liang, J. An, L. Cao, J.C. Xie, and M. Lv, *Ceram. Int.* 43, 14945 (2017).
21. N.J. Lóh, L. Simão, J. Jiusti, A. De Noni Jr, and O.R.K. Montedo, *Ceram. Int.* 43, 8269 (2017).